

# ChemComm

Accepted Manuscript



This is an *Accepted Manuscript*, which has been through the Royal Society of Chemistry peer review process and has been accepted for publication.

*Accepted Manuscripts* are published online shortly after acceptance, before technical editing, formatting and proof reading. Using this free service, authors can make their results available to the community, in citable form, before we publish the edited article. We will replace this *Accepted Manuscript* with the edited and formatted *Advance Article* as soon as it is available.

You can find more information about *Accepted Manuscripts* in the [Information for Authors](#).

Please note that technical editing may introduce minor changes to the text and/or graphics, which may alter content. The journal's standard [Terms & Conditions](#) and the [Ethical guidelines](#) still apply. In no event shall the Royal Society of Chemistry be held responsible for any errors or omissions in this *Accepted Manuscript* or any consequences arising from the use of any information it contains.

## COMMUNICATION

# Synthesis of metalloporphyrin-based conjugated microporous polymer spheres directed by bipyridine-type ligands

Cite this: DOI: 10.1039/x0xx00000x

Guipeng Ji, Zhenzhen Yang, Yanfei Zhao, Hongye Zhang, Bo Yu, Jilei Xu, Huanjun Xu, Zhimin Liu\*

Received 00th January 2012,  
Accepted 00th January 2012

DOI: 10.1039/x0xx00000x

www.rsc.org/

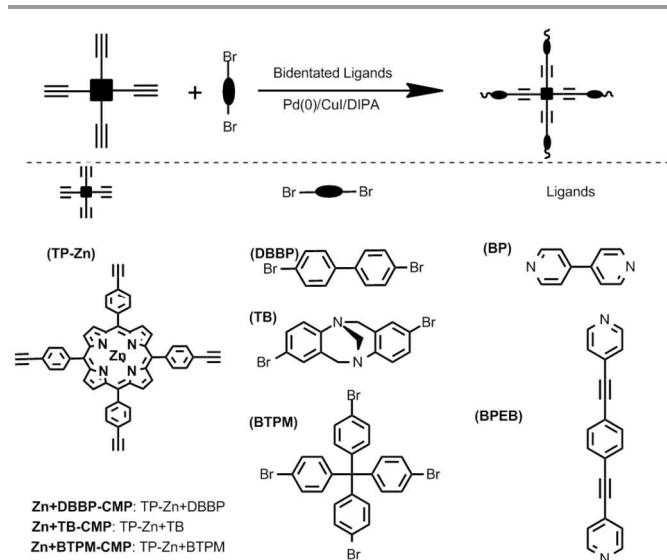
**Zinc porphyrin (TP-Zn) - based conjugated microporous polymer (Zn-CMP) spheres were obtained via Sonogashira–Hagihara cross coupling reactions between 5,10,15,20-tetrakis(4-ethynylphenyl)porphyrin-Zn(II) and sorts of brominated monomers directed by bidentate bipyridine (BP)-type ligands for the first time, and the sphere diameters could be adjusted from 320 to 740 nm. The coordination between BP and TP-Zn was proved to be the key to forming spheres.**

Conjugated microporous polymers (CMPs) are a class of amorphous microporous frameworks with  $\pi$ -conjugated skeletons.<sup>1</sup> Benefit from their high flexibility in molecular design, conjugated skeletons, and ultrahigh surface areas, CMPs have been widely applied in gas adsorption,<sup>2-4</sup> tunable photoluminescence,<sup>5,6</sup> molecular recognition,<sup>3,7,8</sup> light harvesting,<sup>9</sup> photo-catalysis,<sup>10</sup> energy storage<sup>11</sup> and heterogeneous catalysis.<sup>12-14</sup> It is demonstrated that the performances of the CMPs are considerably affected by their morphologies. For example, Deng and co-workers revealed that the phenylethyne-derived CMPs in different morphologies possessed varied Brunauer–Emmett–Teller (BET) surface areas and storage capacity for different solvents.<sup>15</sup> CMP ultrathin films were promising in membrane separation,<sup>16</sup> and showed excellent selectivity, robust reusability and rapid response in chemo- and bio-sensors.<sup>17</sup> Core–shell shaped CMPs displayed color-tunable and controllable light emissions and high luminescence efficiency.<sup>6</sup> Nanotube-like CMPs with unique surface hydrophobicity and porous feature were processed into a bulk absorbent, showing excellent absorption capacity for separation of organics from water.<sup>18</sup> Dispersible metalloporphyrin-based CMP nanoparticles had potential applications in molecular recognition.<sup>7</sup>

Beijing National Laboratory for Molecular Sciences, Key Laboratory of Colloid, Interface and Thermodynamics, Institute of Chemistry, Chinese Academy of Sciences, Beijing 100190, China.  
E-mail: liuzm@iccas.ac.cn.

Electronic Supplementary Information (ESI) available: For experimental details and spectral data. See DOI:

Though CMPs showed morphology-dependent performances, the controllable synthesis of CMPs with specific structures is still a challenge. Template replica strategies<sup>7,16,17,19</sup> or stepwise methods<sup>5,16</sup> have been employed to controllably synthesize CMP networks with specific morphology. However, the tedious operation process and energy-consuming after treatment made it difficult to realize mass production. Hence, development of a convenient, simple operation and easy-handling method for the production of morphology-controllable CMPs materials is still highly desirable. In spite of the fact that polymer spheres have wide applications in devices,<sup>20</sup> carrier,<sup>21</sup> separation,<sup>22</sup> catalysis,<sup>23</sup> controllable synthesis of CMP spheres was seldom reported.<sup>6</sup>



**Scheme 1** Synthetic processes of zinc porphyrin-based CMP networks. DIPA= diisopropylamine. Pd(0)= Pd(PPh<sub>3</sub>)<sub>4</sub>

Herein, we present a simple strategy to prepare size-controllable zinc porphyrin (TP-Zn)-based conjugated microporous polymer (Zn-

CMP) spheres via Sonogashira–Hagihara cross coupling reactions between 5,10,15,20-tetrakis(4-ethynylphenyl)porphyrin-Zn(II) (TP-Zn) and brominated monomers directed by bidentate ligands including bipyridine (BP) and 1,4-bis(pyridin-4-ylethynyl)benzene (BPEB) under air or N<sub>2</sub> atmosphere (Scheme 1). As a result, dispersible and uniform (polydispersion index < 0.2) Zn-CMP spheres with diameters varying from 320 to 740 nm (hydrodynamic diameters by dynamic light scattering (DLS) method) were successfully obtained.

The coupling reaction between TP-Zn and 2,8-dibromo-6H,12H-5,11-methanodibenzo[b,f]diazocine (TB) was carried out under different conditions (Table S1, ESI), and the resultant samples were characterized by means of different techniques. Solid-state <sup>13</sup>C cross-polarization magic angle spinning (CP/MAS) NMR was applied to characterize the chemical structure of CMP spheres. The signals ranging from 119 to 150 ppm were assigned to the aromatic carbon from Zn-porphyrin and TB in the CMP spheres, and those from 75 to 91 ppm were assigned to the C-C triple bond sites from Zn-porphyrin (Figure S1, ESI). The signals at 62 to 64 ppm represented the benzyl carbon in TB of CMP spheres, respectively. <sup>13</sup>C-NMR showed the monomers were well fabricated into the skeleton of the polymer spheres. The peaks at 1000 cm<sup>-1</sup> and 2180 cm<sup>-1</sup> in the Fourier transform infrared (FT-IR) spectra (Figure S8) presented the N-Zn in-plane bending and alkyne's characteristic bands, respectively, which also indicated the successful coupling reaction.

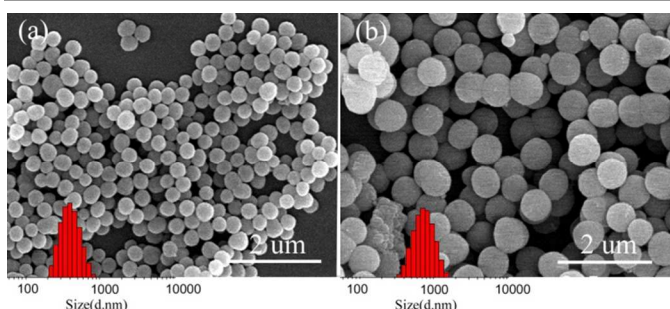


**Figure 1** Typical SEM images of the Zn+TB-CMP spheres obtained under mild condition: (a) at 0°C, N<sub>2</sub>, (b) at 25°C, air.

The morphology of the resultant CMPs were observed via scanning electron microscopy (SEM). To our delight, monodispersible and uniform Zn+TB-CMP spheres were obtained in the presence of BP, as illustrated in Figure 1, while the resultant Zn+TB-CMPs were in irregular chunk bodies in the absence of BP (Figures S2a). For comparison, pyridine as a monodentate ligand and BPEB as another bidentate ligand were used in the synthesis processes, respectively. It was demonstrated that the presence of BPEB also directed the formation of Zn-CMP spheres (Table S1, entry 12), while no spheres were obtained with pyridine (Table S1, entry 11). In a control experiment, BP was added into the reaction system after the formation of Zn+TB-CMP, however, no spheres were obtained (Table S1, entry 7), suggesting that the resultant Zn+TB-CMP spheres were not formed via the reconstruction of Zn+TB-CMP bulk bodies. The influence of the reaction solvents on the morphology of CMPs was investigated, and it was found that chloroform (CHCl<sub>3</sub>) was the best solvent for forming Zn+TB-CMP spheres with uniform size (Figure 1), and other tested solvents including toluene, tetrahydrofuran (THF)

and 1,4-dioxane were unfavourable to the formation of the spheres (Figures S2b-c).

In the respect of controlling the size of the spheres, it was indicated that the sphere size increased with temperature under the air atmosphere (Figure S3). For example, at 0°C, the hydrodynamic diameter was centred about 360 nm, and it became larger up to about 560 and 740 nm as the temperature rose to 20 and 25°C, respectively. While, under the N<sub>2</sub> atmosphere the average size of spheres obtained at 0°C was about 400 nm, slightly larger than that of those obtained at 25°C (350 nm) (Figures S4a-b). Other factors, such as, stirring speed, concentration of monomers (Figure S4c), and the appropriate proportion between ligands and TP-Zn (Table S1, entry 9, 13) were proved to have little influence on the average sphere size. It was noteworthy that similar CMP spheres were obtained via the condensation between TP-Zn and 4,4'-dibromobiphenyl (DBBP) or and tetrakis(4-bromophenyl)methane (BTPM) under the N<sub>2</sub> atmosphere (Figures S5a-b), which showed great potential in terms of structural design of CMPs with various functional sites.

According to the contrast tests (Table S1, entry 2, 6, 11, 12, Table S2, entry 1), both TP-Zn and the bidentate ligands (i.e., BP and BPEB) were essential for the formation of the Zn-CMP spheres. To explore the possible sphere-forming mechanism, the mixture of TP-Zn and BP (2:1) was analysed by NMR. From the <sup>1</sup>H-NMR spectra (Figure 2a), it was clear that the proton of BP downfield shifted from 8.75 to 7.0 ppm for H-1 and from 7.54 to 6.8 ppm for H-2, respectively, suggesting the strong coordination between BP and TP-Zn, consistent with previous reports.<sup>24,25</sup> The similar shift of the proton of BP was also observed in the <sup>1</sup>H-NMR spectra of the time-dependent reaction solution (Figure S10, o h). These results demonstrated the coordination between BP and TP-Zn was the key to forming spheres.

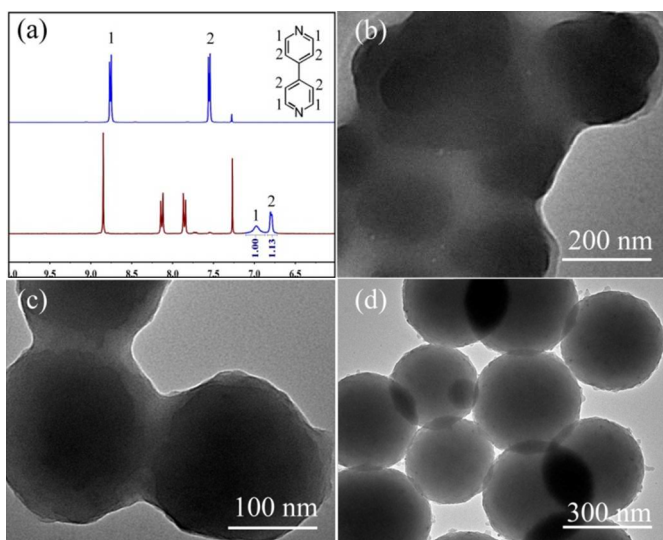


**Figure 2** (a) <sup>1</sup>H-NMR spectra of 4,4'-bipyridine (up) and BP:TP-Zn=1:2(down), TEM images of the spherical Zn+TB-CMP obtained at reaction time of (b) 1 h, (c) 4 h, (d) 12 h (BP, CHCl<sub>3</sub>, 25°C, N<sub>2</sub>).

Transmission electron microscopy (TEM) was used to track the morphology changes in the CMPs time-dependently obtained via Sonogashira-Hagihara coupling reaction with (Figures 2b-d) and without bipyridine (Figure S9). From the morphology changes in the

CMPs obtained at different reaction time, we speculated the possible formation mechanism of CMP spheres as follows. In the presence of BP, monomers or oligomers with Zn-center in low coupling degree (containing lots of unreacted sites) formed at the beginning were pulled together through coordination effect, resulting in obvious aggregation (1h, Figure 2b). Then, more and more monomer molecules were integrated and CMPs with higher coupling degree were formed gradually (1-12h, Figures 2c-d). Compared with other morphology, the spherical structure had the lowest surface Gibbs free energy, which was probably the driving force to form CMP spheres in our system. In contrast, in the case without bipyridine ligand, the CMP aggregates merely formed via coupling reaction were randomly dispersed in the reaction system, leading to irregular bulk bodies at last.

It was worth noting that the content of the residual bipyridine was 97% in the reaction solution after completion of the reaction, suggesting that almost no bipyridine was wrapped in the obtained CMP spheres. This was also proved by the  $^1\text{H-NMR}$  spectra of the time-dependent reaction solutions, which showed the peaks assigning to BP disappeared in the spectrum of the solution at 2 h and appeared again at 12 h (Figure S10). It may be explained as follows. Along with the formation of CMP polymers, the increasing steric hindrance and changes in the electronic effect around the Zn-center may weaken the coordination effect, thus leading to the release of the BP ligand.

Based on the above results, it could be deduced that the coordination of BP with TP-Zn was the key to the formation of CMPs. This could explain the influence of the solvents on the morphologies of Zn-CMPs.  $\text{CHCl}_3$  cannot coordinate with TP-Zn, and has suitable solvent power to dissolve TP-Zn, while THF or 1,4-dioxane can coordinate with TP-Zn, which may interfere the coordination of BP with TP-Zn, thus inhibiting the formation of Zn-CMPs.

To explore the reasons for the growth of CMP spheres at higher temperature under air condition, the oxidative couplings of TP-Zn were carried out (Table S2, entry 2-4). It was indicated that the oxidative coupling hardly proceeded without  $\text{O}_2$  or at  $0^\circ\text{C}$  and proceeded successfully along with the temperature in the presence of  $\text{O}_2$ . This result was well consistent with the trend of the changes in CMP spheres, which changed little under  $\text{N}_2$  or at  $0^\circ\text{C}$  and became bigger along with the temperature in the presence of  $\text{O}_2$ . Therefore, we believed the growth of CMP spheres was caused by the oxidative coupling reaction.

Kinds of methods were applied to character the CMP spheres. The Zn-CMP spheres obtained were completely insoluble in conventional solvents, such as THF,  $\text{CHCl}_3$ , methanol, DMSO and DMF. Element analysis showed the Zn contents were 5.30%, 5.03%, 4.96% for Zn+DBBP-CMP, Zn+TB-CMP, Zn+BTPM-CMP, respectively, which were slightly lower than the theoretical amounts, probably due to the unreacted Br sites. Thermo-gravimetric analysis (TGA) results (Figure 3a) showed the exceptional thermal stability of Zn-CMP spheres, which didn't decompose before  $380^\circ\text{C}$ , and Zn+DBBP-CMP spheres were stable even up to  $420^\circ\text{C}$ . The porosity of CMP spheres were measured by nitrogen sorption analysis at 77 K. The type I-like  $\text{N}_2$  sorption isotherms (Figures 3b-d) and the pore size distribution (Figure S7, ESI) indicated the microporous structure of the resultant polymers. Because of the similar twisted structure of brominated monomers, the Zn+TB-CMP and the Zn+BTPM-CMP spheres had

similar pore size distribution, with the average pore size centering at 0.78 nm (Figure 3c, S7) and 0.82 nm (Figure 3d, S7), respectively. However, Zn+DBBP-CMP spheres had a larger average pore size at 1.69 nm (Figures 3b, S7), which may be ascribed to the liner structure of the brominated monomer. The Brunauer–Emmett–Teller (BET) surface areas of these Zn-CMP spheres reached up to  $650\text{ m}^2\text{g}^{-1}$  (Table S1, entry18),  $479\text{ m}^2\text{g}^{-1}$  (Table S1, entry 14) and  $37\text{ m}^2\text{g}^{-1}$  for Zn+BTPM-CMP, Zn+TB-CMP and Zn+DBBP-CMP, respectively (Figure S6, ESI).

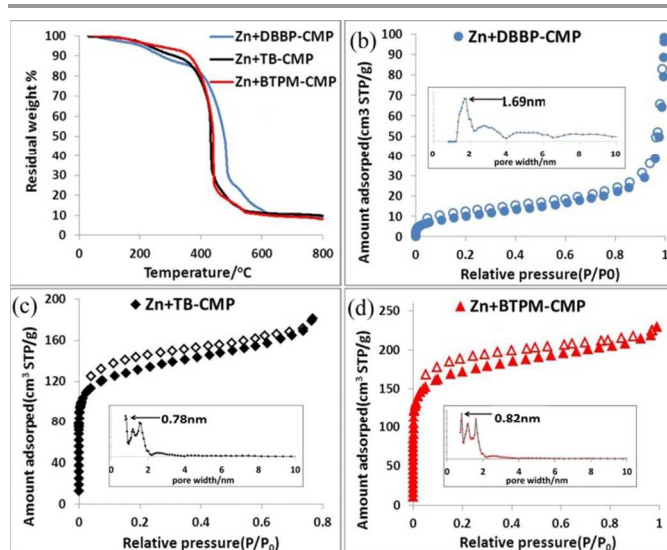


**Figure 3** (a) Thermogravimetric analysis (TGA). Adsorption (filled) and desorption (empty) isotherms of  $\text{N}_2$  at 77 K for CMP spheres and their pore size distribution through NLDFT method. (b) Zn+DBBP-CMP (c) Zn+TB-CMP (d) Zn+BTPM-CMP.

In summary, Zn-CMP spheres in diameter from 320 nm to 740 nm were prepared via Sonagashira–Hagihara cross coupling reaction directed by the bipyridine-type ligands under mild conditions. The coordination between TP-Zn and the bidentate ligands was essential for the formation of Zn-CMP spheres and oxidative coupling affected the diameters of the resultant spheres. This strategy was quite convenient in terms of handling and separation, and was applicable to sorts of halogenate monomers, which was significant in preparing functional CMP spheres in large scale. Given the universality of coordination in chemistry and the structural diversity of CMPs, we expected this work could provide a new route to preparing dispersible and uniform functional CMP spheres.

## References

- 1 Y. Xu, S. Jin, H. Xu, A. Nagai and D. L. Jiang, *Chem. Soc. Rev.*, 2013, **42**, 8012-8031.
- 2 X. Liu, Y. Xu, Z. Guo, A. Nagai and D. L. Jiang, *Chem. Commun.*, 2013, **49**, 3233-3235.
- 3 Y. Zhang, S. A. Y. Zou, X. Luo, Z. Li, H. Xia, X. Liu and Y. Mu, *J. Mater. Chem. A*, 2014, **2**, 13422-13430.
- 4 Q. Chen, D. P. Liu, M. Luo, L. J. Feng, Y. C. Zhao and B. H. Han, *Small*, 2014, **10**, 308-315.
- 5 Y. Xu, L. Chen, Z. Guo, A. Nagai and D. L. Jiang, *J. Am. Chem. Soc.*, 2011, **133**, 17622-17625.
- 6 Y. Xu, A. Nagai and D. L. Jiang, *Chem. Commun.*, 2013, **49**, 1591-1593.

- 7 K. Wu, J. Guo and C. Wang, *Chem Commun (Camb)*, 2014, **50**, 695-697.
- 8 X. Liu, Y. Xu and D. L. Jiang, *J. Am. Chem. Soc.*, 2012, **134**, 8738-8741.
- 9 L. Chen, Y. Honsho, S. Seki and D. L. Jiang, *J. Am. Chem. Soc.*, 2010, **132**, 6742-6748.
- 10 J. X. Jiang, Y. Li, X. Wu, J. Xiao, D. J. Adams and A. I. Cooper, *Macromolecules*, 2013, **46**, 8779-8783.
- 11 Y. Kou, Y. Xu, Z. Guo and D. L. Jiang, *Angew. Chem. Int. Ed.*, 2011, **50**, 8753-8757.
- 12 Y. Xie, T. T. Wang, X. Liu, K. Zou and W. Q. Deng, *Nat. Commun*, 2013, **4**, 1960.
- 13 Z. Z. Yang, Y. Zhao, H. Zhang, B. Yu, Z. Ma, G. Ji and Z. Liu, *Chem. Commun.*, 2014, **50**, 13910-13913.
- 14 Y. Zhang, Y. Zhang, Y. L. Sun, X. Du, J. Y. Shi, W. D. Wang and W. Wang, *Chem. Eur. J.*, 2012, **18**, 6328-6334.
- 15 D. Tan, W. Fan, W. Xiong, H. Sun, Y. Cheng, X. Liu, C. Meng, A. Li and W. Q. Deng, *Macromol. Chem. Phys.*, 2012, **213**, 1435-1440.
- 16 M. Kim, M. Byeon, J. S. Bae, S. Y. Moon, G. Yu, K. Shin, F. Basarir, T. H. Yoon and J. W. Park, *Macromolecules*, 2011, **44**, 7092-7095.
- 17 C. Gu, N. Huang, J. Gao, F. Xu, Y. Xu and D. L. Jiang, *Angew. Chem. Int. Ed. Engl.*, 2014, **53**, 4850-4855.
- 18 W. Fan, X. Liu, Z. Zhang, Q. Zhang, W. Ma, D. Tan and A. Li, *Micropor. Mesopor. Mater.*, 2014, **196**, 335-340.
- 19 G. X. Li, Y. L. Li, H. B. Liu, Y. B. Guo, Y. J. Li and D. B. Zhu, *Chem. Commun.*, 2010, **46**, 3256-3258.
- 20 K. Tabata, D. Braam, S. Kushida, L. Tong, J. Kuwabara, T. Kanbara, A. Beckel, A. Lorke and Y. Yamamoto, *Sci. Rep.*, 2014, **4**, 5902.
- 21 P. F. Gao, L. L. Zheng, L. J. Liang, X. X. Yang, Y. F. Li and C. Z. Huang, *Journal of Materials Chemistry B*, 2013, **1**, 3202-3208.
- 22 L. Liu, Q. F. Deng, X. X. Hou and Z. Y. Yuan, *J. Mater. Chem.*, 2012, **22**, 15540-15548.
- 23 M. Choudhary, R. U. Islam, M. J. Witcomb, M. Phali and K. Mallick, *Appl. Organomet. Chem.*, 2013, **27**, 523-528.
- 24 M. C. O'Sullivan, J. K. Sprafke, D. V. Kondratuk, C. Rinfray, T. D. Claridge, A. Saywell, M. O. Blunt, J. N. O'Shea, P. H. Beton, M. Malfois and H. L. Anderson, *Nature*, 2011, **469**, 72-75.
- 25 B. Zhu, H. Chen, W. Lin, Y. Ye, J. Wu and S. Li, *J. Am. Chem. Soc.*, 2014, **43**, 15126-15129.
- 26 Q. Lin, J. Lu, Z. Yang, X. C. Zeng and J. Zhang, *J. Mater. Chem. A*, 2014, **2**, 14876-14882.